



## Application value of Co(II) coordination polymer in the treatment and operational nursing of hypothermia

Sha Li<sup>a</sup>, Ye Li<sup>b</sup> & Fang-Yu Zhou<sup>a,\*</sup>

<sup>a</sup>Anesthesia Operation Department, Guangrao County People's Hospital, Dongying, Shandong, China

<sup>b</sup>Oncology Department, Shandong Public Health Clinical Center (Jinan infectious Disease Hospital), Jinan, Shandong, China

\*E-mail: olcjsvlt042265@163.com

Received 28 August 2021; revised and accepted 16 November 2021

A novel coordination polymer,  $[\text{Co}_3(\text{OABDC})_2(\text{bipy})_3(\text{H}_2\text{O})_6]_n(\text{CH}_3\text{OH})_n(\text{H}_2\text{O})_{4.5n}$  (**1**), has been synthesised by hydrothermal method with the coordination of 4,4'-bipy ligand and 3,5-dicarboxyphenoxyacetic acid ( $\text{H}_3\text{OABDC}$ ) to cobalt(II) ions. The treatment and nursing application values of **1** on hypothermia in patients undergoing surgery has been examined, and the specific mechanism is explored. The application of the compound on the body temperature is measured with an *in vitro* infrared thermometer. Then, the relative expression of vascular  $\alpha$ -receptors is determined by real-time RT-PCR. The toxicity and biocompatibility of the new compound is also determined.

**Keywords:** Coordination polymer, Hypothermia, Laparoscopic cholecystectomy

Hypothermia during surgery may inhibit the body's immunity, especially the oxidative lethality of neutrophils, as well as reduce skin blood flow and the tissue absorption of oxygen<sup>1</sup>. Hypothermia during surgery may also increase protein consumption and reduce bone keratin synthesis. It is a non-negligible factor leading to incision infection<sup>2</sup>.

Coordination polymers are receiving extensive attention because of their abundant structures and applications in guest exchange, catalysis, adsorption, optic materials, magnetism, etc. For coordination polymers, their assembly is affected by various key factors, such as solvent, temperature, pH, and reactant concentration, together with some internal factors, such as the central-metal coordination geometry and the organic ligands' flexibility and configuration<sup>3-7</sup>. Designing organic ligands and/or adjusting the conditions of synthesis are important to acquire the target skeletons with specific functions and structures<sup>8,9</sup>. To achieve infinite structure extension, organic ligands having two or more coordination atoms (e.g., S, O, and N atoms) are usually used. Multi carboxylic acids are the most extensively used connectors to assemble various coordination polymers<sup>10-12</sup>. They can utilize different coordination patterns to meet the needs of central-metal coordination geometry, thereby forming distinct multidimensional structures. Furthermore, the

existence of the extra nitrogen-donor ligand could further extend the structure and enhance the framework robustness<sup>13-18</sup>. In the present study, a new coordination polymer,  $[\text{Co}_3(\text{OABDC})_2(\text{bipy})_3(\text{H}_2\text{O})_6]_n(\text{CH}_3\text{OH})_n(\text{H}_2\text{O})_{4.5n}$  (**1**), was produced by a hydrothermal method through the coordination of 4,4'-bipy and 3,5-dicarboxyphenoxyacetic acid ( $\text{H}_3\text{OABDC}$ ) by using cobalt(II) nitrate. The structure of compound **1** was characterised by elemental analysis, thermo gravimetric analysis (TGA), infrared (IR) spectroscopy, and single-crystal diffraction. In the crystal of  $\text{H}_3\text{OABDC}$ , it linked metal nodes to generate two-dimensional (2D) wavy-layer structures, and then the ligand of 4,4'-bipy linked the wavy layers to create a three-dimensional (3D) porous skeleton via the double-helix coordination. Regarding the biological aspect, the treatment and nursing application values of this novel compound for hypothermia in patients undergoing surgery were evaluated.

### Materials and Methods

#### Chemicals and measurements

The reagents passed the quality analysis and were thus used as received. TENSOR 27 spectrometer was used to record the IR spectra between 400 and 4000  $\text{cm}^{-1}$ . To investigate the elemental composition

of carbon, nitrogen, and hydrogen, a PerkinElmer 2400LS II was used. Smartlab 9 was applied to acquire the patterns of PXRD utilizing Cu K $\alpha$  radiation ( $\lambda = 1.5418 \text{ \AA}$ ). At 25 and 800 °C, by utilizing a TA Q600, TGA was conducted at an increase rate of 10 °C per min under air flow. A U-3900H spectrophotometer was used to obtain ultraviolet–visible absorption spectra.

**Preparation and characterization of [Co<sub>3</sub>(OABDC)<sub>2</sub> (bipy)<sub>3</sub>(H<sub>2</sub>O)<sub>6</sub>]<sub>n</sub>(CH<sub>3</sub>OH)<sub>n</sub>(H<sub>2</sub>O)<sub>4.5n</sub> (1)**

NaOH (0.2 mmol), 4,4'-bipyridine (0.1 mmol), and H<sub>3</sub>OABDC (0.1 mmol) were layered in a solution (6 mL) containing 4 mL of water and 2 mL of methanol. Furthermore, a solution (6 mL) containing 4 mL of water, 2 mL of ethanol, and Co(NO<sub>3</sub>)<sub>2</sub>·6H<sub>2</sub>O (0.2 mmol) was dropwise added slowly with stirring. This solution was then placed in a stainless-steel reactor (25 mL) with polytetrafluoroethylene lining and it heated for 72 h at 160 °C. After cooling to room temperature at a rate of 2 °C·h<sup>-1</sup>, massive pink crystals were obtained at 32% yield (calculated via H<sub>3</sub>OABDC). Elemental analysis was on the basis of C<sub>51</sub>H<sub>57</sub>Co<sub>3</sub>N<sub>6</sub>O<sub>25.5</sub>. Calcd. (%) N, 6.28; H, 4.29; C, 45.75; Found (%): N, 6.59; H, 3.12; and C, 45.69. IR (KBr, cm<sup>-1</sup>, Fig S1, Supplementary Data): 3403 w, 3124 m, 3114 w, 2931 w, 1552 s, 1506 w, 1403 m, 1342 w, 1289 m, 1147 m, 1000 w, 771 w, 670 w..

An Oxford Xcalibur E diffractometer was used to obtain X-ray data. CrysAlisPro was utilized to determine the strength data, which were subsequently converted to HKL files. The direct-mean-based SHELXS program and the least-square-method-based SHELXL-2014 were used to create and modify the original structural modes, respectively. The anisotropic parameters were mixed after using entire non-H atoms. Eventually, entire H-atoms were fixed on the C atoms, to which they were geometrically linked using AFIX commands. The optimization details of the compound and parameters of crystallography are listed in the Table 1. The selected bond lengths and angles are listed in Tables S1 and S2 (Supplementary Data).

**Body-temperature measurement**

An *in vitro* infrared thermometer was used to measure the body temperature of the animal received with surgery. This research was completed strictly following the instructions' guidance accompanied with minor modifications. Fifty BALB/C mice (weighing 200–220 g; aged 6–8 weeks), provided by the Model Animal Center of Nanjing University, were

used in this research. All procedures were authorized by the Animal Ethics Committee of Nanjing University. All animals were separated into the following groups: compound-treatment, control, and model groups. Then, laparoscopic cholecystectomy was performed on the animal from the model and treatment groups. Subsequently, treatment with **1** was accomplished at 1, 2, and 5 mg/kg concentrations. After the indicated treatment, the *in vitro* infrared thermometer was used to measure the body temperature of the animal.

**Real-time RT-PCR**

To detect the influence of as-prepared compound on the relative expression of the vascular  $\alpha$ -receptors of the animal received with surgery and compound treatment, real time RT-PCR was performed based on the instructions with some modifications. Fifty BALB/C mice (weighing 200–220 g; aged 6–8 weeks), provided by the Model Animal Center of Nanjing University, were used. All procedures were authorized by the Animal Ethics Committee of Nanjing University. All animals were separated into the following groups: compound-treatment, control, and model groups. Laparoscopic cholecystectomy

Table 1 — Optimization details and crystallography parameters of the compound

Empirical formula	C <sub>102</sub> H <sub>114</sub> Co <sub>6</sub> N <sub>12</sub> O <sub>51</sub>
Formula weight	2677.62
Temperature (K)	298.15
Crystal system	monoclinic
Space group	C2/c
a (Å)	17.326(2)
b (Å)	15.148(3)
c (Å)	23.1129(17)
$\alpha$ (°)	90
$\beta$ (°)	96.957(2)
$\gamma$ (°)	90
Volume (Å <sup>3</sup> )	6021.4(15)
Z	2
$\rho_{\text{calc}}$ (g/cm <sup>3</sup> )	1.477
$\mu$ (mm <sup>-1</sup> )	0.903
Reflections collected	13846
Independent reflections	5097 [R <sub>int</sub> = 0.0833, R <sub>sigma</sub> = 0.1144]
Data/restraints/parameters	5097/6/404
Goodness-of-fit on F <sup>2</sup>	1.023
Final R indexes [I >= 2 $\sigma$ (I)]	R <sub>1</sub> = 0.0615, $\omega$ R <sub>2</sub> = 0.1468
Final R indexes [all data]	R <sub>1</sub> = 0.1110, $\omega$ R <sub>2</sub> = 0.1700
Largest diff. peak/hole (e Å <sup>-3</sup> )	0.58/-0.42
CCDC	2102197

was performed on the animal from the model and treatment groups. Subsequently, treatment was performed by adding compound **1** at 1, 2, and 5 mg/kg concentrations. Vascular endothelial cells were then harvested, and entire RNA was extracted from cells by using TRIzol Reagent following the manufacturer's instructions. OD260/OD280 ratio was used to measure the entire RNA concentration, followed by reverse transcription into the cDNA by using a cDNA reverse transcription kit with high capacity. Finally, SYBR Green Master Mix was applied to test  $\alpha$ -receptors' relative expression after treatment with the as-synthesized compound. We used the  $2^{-\Delta Ct}$  approach to carry out relative quantification three times.

#### CCK-8 assay

CCK-8 assay was conducted to measure the toxicity of the new compound on human vein endothelial cells. This preformation was conducted completely under the guidance of protocols with only minor modifications<sup>19</sup>. In a typical procedure, human vein endothelial cells in the logical growth phase were collected and seeded onto 96-well plates at a concentration of 5000 cells/well. All cells were cultured in an incubator at 37 °C and 5% CO<sub>2</sub> for 12 h. Then, the compound was added for the indicated treatment with a series of different concentrations. After discarding the cell-culture medium, fresh medium containing CCK-8 reagent was used for further incubation. Finally, cytotoxicity was evaluated according to the manufactures' standard.

#### Hemolysis toxicity

The hemolysis toxicity of the new compound was also evaluated completely under the guidance of the instructions with some modifications<sup>20</sup>. In a typical procedure, the blood used in the hemolysis experiment was collected from adult male New Zealand white rabbits, which were obtained from the Model Animal Center of Nanjing University. The compound was added into the well and then incubated at 37 °C. The rabbit blood was then added into the well for further incubation. The supernatant was transferred into a cuvette, and absorbance at 545 nm was measured using a spectrophotometer. The *in vitro* hemolysis of the compound was determined by measuring red blood cell lysis and hemoglobin release.

## Results and Discussion

### Structural characterization

According to the structural analysis of X-ray crystals, compound **1** belongs to the monoclinic space

group of *C2/c*. The crystallography of **1** is summarized in Table 1. The fundamental unit of **1** (Fig. 1a) was constructed from the two metal centers of Co2 and Co1, a totally deprotonated OABDC<sup>3-</sup>, two molecules of 4,4'-bipy, three coordinated molecules of H<sub>2</sub>O, and three ionized molecules of H<sub>2</sub>O. Fig. 1a shows that Co1 ions were six-coordinated, with two oxygen atoms belonging to the carboxyl directly bridged onto the benzene ring provided by two ligands (nitrogen atoms on two ligands of 4,4'-bipy and oxygen atoms on two-coordinated molecules of H<sub>2</sub>O), thereby producing a deformed octahedron structure. Co2 ions were also six-coordinated, with an oxygen atom on the benzoic acid derived from a ligand and the carboxylic acid oxygen on aryloxyacetic acid originating from another ligand, and two nitrogen atoms provided by two ligands of 4,4'-bipy and oxygen belonging to two-coordinated molecules of H<sub>2</sub>O, thereby generating a deformed octahedron structure. The four neighbouring metal cores of Co2, Co1, Co2', and Co1' in the skeleton created a parallelogram. In the crystal structure, the 4,4'-bipy ligand bridged the metal nodes to generate a 3D porous skeleton, and the H<sub>3</sub>OABDC linked metal nodes to produce 2D wavy-layer structures (Figs. 1b and 1c). The porous diameters were approximately 16.030 Å × 15.289 Å and 15.914 Å × 15.289 Å, respectively. In the unit cell, total solvent-accessible volume of the channel was 90.8 Å<sup>3</sup>, accounting for 1.5% of the overall cell volume after PLATON calculation. Numerous H bonds existed in **1**, increasing its stability. The entire skeleton of the compound could be regarded as a 3,4,4-bridged network by regarding the Co ions as four-linked nodes and H<sub>3</sub>OABDC as a three-linked node (Fig. 1d).

To examine the phase purity of the products, PXRD patterns of **1** were obtained (Fig. 2a). The peak positions of experimental patterns were consistent with those of the simulation ones, indicating that the crystal structure represented the products of massive crystals. The strength differences may be due to the preferred selection of the crystal sample. Thermal decomposition of compound **1** was detected at 10 °C·min<sup>-1</sup> increase rate under nitrogen flow. Fig. 2b shows that the TG curve had a weight loss for the first time between 57.6 and 258.4 °C, with 16.58% ratio of weight loss (16.44% calculated value), revealing a loss of methanol molecules, free H<sub>2</sub>O, and coordinated molecules of H<sub>2</sub>O. The second weight loss occurred between 365.6 and 728.7 °C, with a

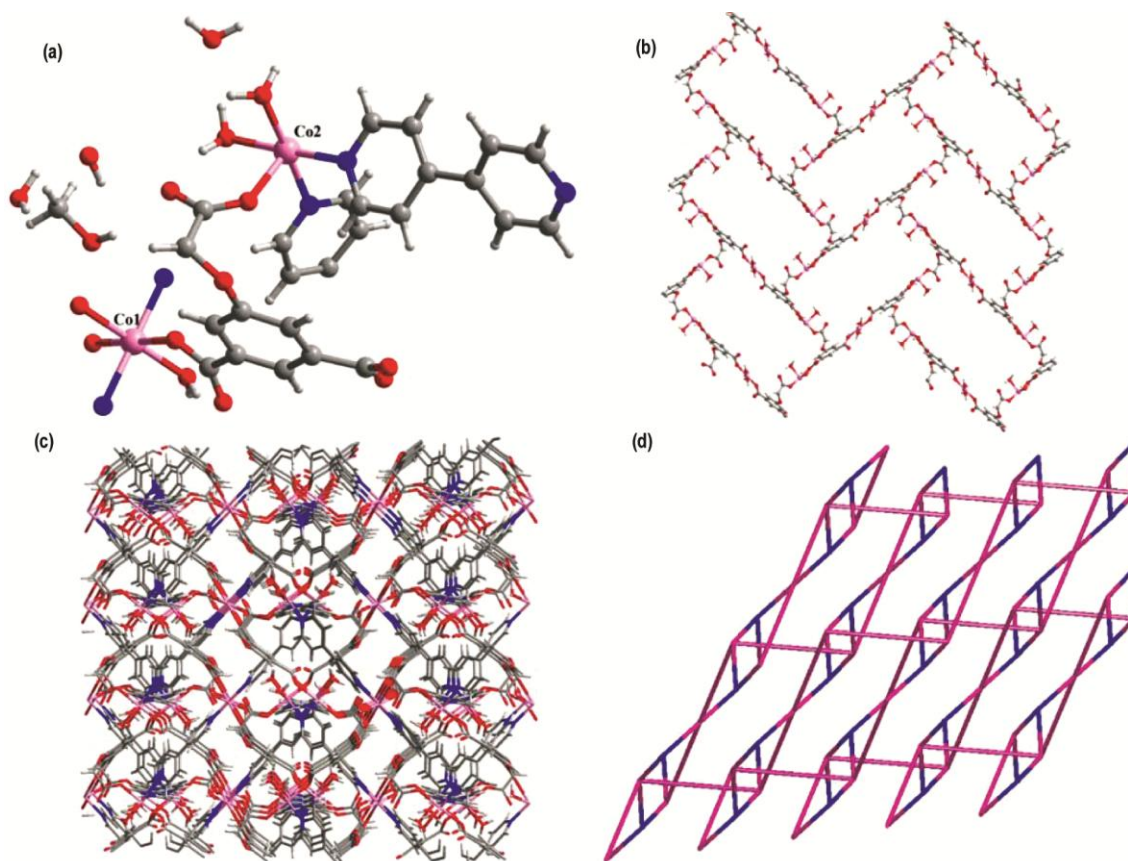


Fig. 1 — (a) Coordination environment for Co(II) ion, (b) two-dimensional co-carboxylic acid layer, (c) Three-dimensional diagram and (d) the 3,4,4-bridged network of compound **1**

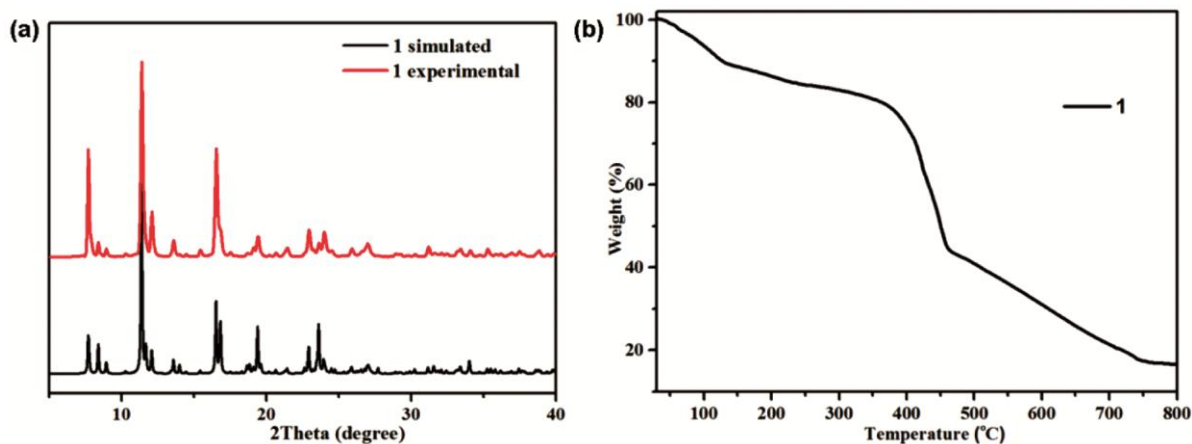


Fig. 2 — (a) PXRD patterns and (b) TGA curve of compound **1**

weight-loss ratio of 66.47% (66.86% calculated value), indicating ligand decomposition and metal-organic skeleton conversion to carbon and metal oxides. The remaining amount of CoO was 20.95% (16.72% calculated value).

In the IR spectra of compound **1**, the absorption band at  $3403\text{ cm}^{-1}$  can be assigned to the stretching

vibration of hydroxyl (O–H) group, suggesting the presence of water molecules in **1**. The weak bands at  $3124$  and  $3114\text{ cm}^{-1}$  can be assigned to  $\nu(\text{Ar-H})$  of the ligands. The IR bands at  $2931\text{ cm}^{-1}$  can be attributed to the  $\nu(\text{C-H})$  of methyl group in lattice MeOH molecule. The characteristic bands of carboxyl groups in **1** are shown at  $1552$  and  $1403\text{ cm}^{-1}$ . The respective

values of ( $\nu_{\text{asym}}(\text{COO}^-)-\nu_{\text{sym}}(\text{COO}^-)$ ) ( $149\text{ cm}^{-1}$ ) suggest the presence of chelating coordination mode of the carboxylate groups. The absence of the expected absorption bands at around  $1700\text{ cm}^{-1}$  for the protonated carboxyl group indicates that all carboxyl groups of  $\text{H}_2\text{Pim}$  have been deprotonated. The bands at  $1342$  and  $1289\text{ cm}^{-1}$  as well as those from  $1000$  to  $670\text{ cm}^{-1}$ , should be attributed to the bipy ligands. These spectral informations are consistent with the results of the single-crystal X-ray diffraction analyses.

**Prevention of hypothermia in patients during surgery**

After preparing the novel compound, its biological activity was examined. The prevention against the body temperature by using the compound was measured with an *in vitro* infrared thermometer.

Fig. 3 shows that the model group had a much lower temperature than the control group. The model and control groups remarkably differed. After the treatment with the compound, the animal's temperature was increased. The biological activity of the new compound exhibited a dose-dependent manner.

**Inhibition of the expression of vascular  $\alpha$ -receptors**

In the previous experiment, we confirmed the as-created excellent biological activity of the compound against hypothermia in patients during surgery. As vascular  $\alpha$ -receptors play critical roles in thermoregulation, we performed real-time RT-PCR to measure the relative expression of the vascular  $\alpha$ -receptor. Fig. 4 shows that the expression of  $\alpha$ -receptors was lower in the model group than in the

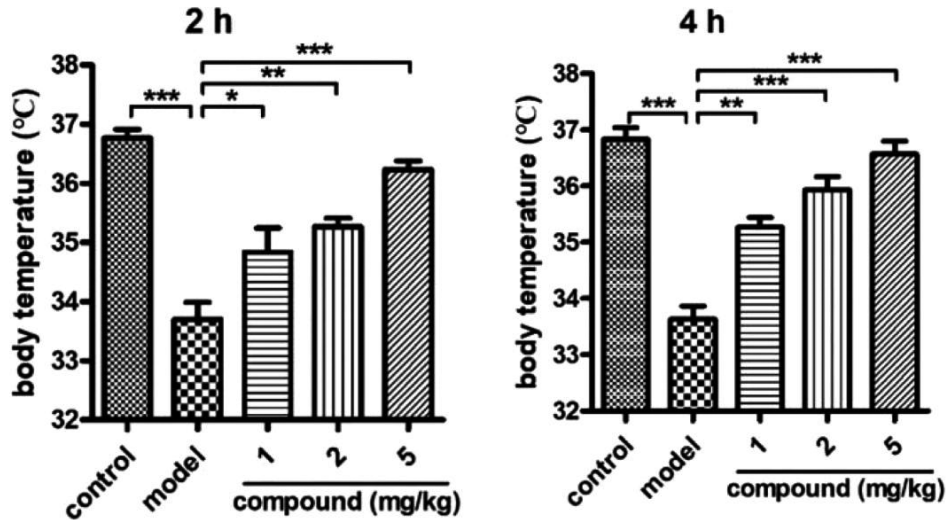


Fig. 3 — Plots for Compound 1 showing prevention of hypothermia in patients during surgery

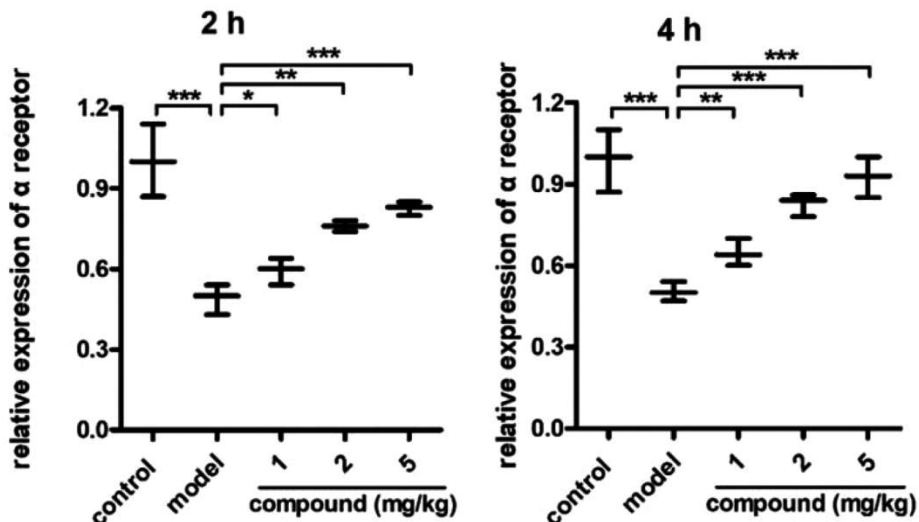


Fig. 4 — Plots for relative expression of  $\alpha$ -receptor with different concentration of compound 1

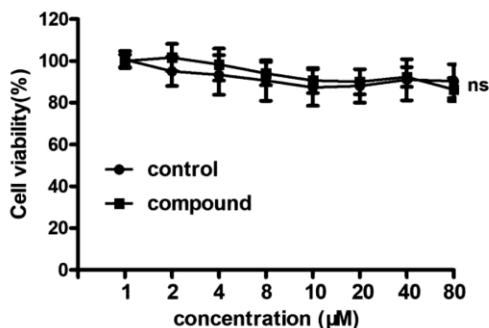


Fig. 5 — Plots for cell viability with different concentration of compound 1

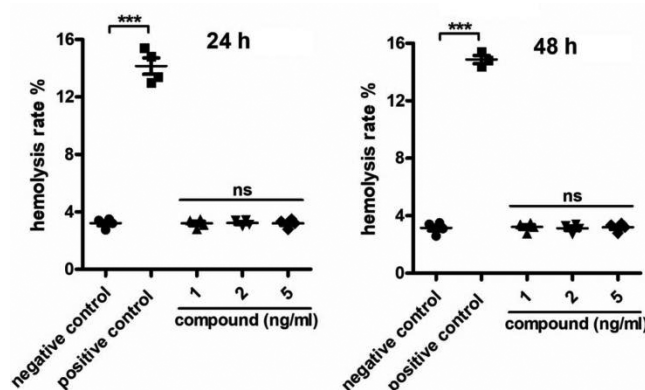


Fig. 6 — Plots for hemolysis rate with different concentration of compound 1

control group. Nevertheless, after treating with the as-prepared complex,  $\alpha$ -receptor expression significantly increased in a dose-dependent manner.

#### Effect of compound 1 on human vein endothelial cells

As described above, compound 1 had excellent biological application in hypothermia in patients during surgery by decreasing the relative expression of vascular  $\alpha$ -receptors. However, Co(II) metal is toxic, and the toxicity of the new compound on human vein endothelial cells also needed to be evaluated. Thus, CCK-8 assay was conducted, and the inhibitory activity of the new compound on viability of human vein endothelial cells was measured. Results are shown in Fig. 5. Compared with normal cells, the compound showed no influence on the viability of human vein endothelial cells, suggesting the excellent application value of the new compound during treatment.

#### Biocompatibility of compound 1

In the above experiments, we proved that compound 1 had excellent biological application in

hypothermia in patients during surgery, as well as low toxicity on human vein endothelial cells. Additionally, the biocompatibility of the new compound was evaluated. Results are shown in Fig. 6. The positive control group had a much higher level of hemolysis rate, which was significantly reduced by the new compound. This inhibition ability of the new compound did not significantly differ from that of the negative control group ( $P > 0.05$ ).

#### Conclusions

We synthesized a new compound, Co(II)-CP, through a hydrothermal method by coordinating 4,4'-bipy and 3,5-dicarboxyphenoxyacetic acid and applying cobalt(II) nitrate. The structure of the compound was characterized by TGA, EA, IR spectroscopy, and single-crystal diffraction techniques. The crystal of  $H_3OABDC$  linked metal nodes to generate 2D wavy-layer structures, whereas the ligand of 4,4'-bipy linked these wavy layers to create a 3D porous skeleton via the double-helix coordination. The temperatures obtained using an *in vitro* infrared thermometer showed that the compound prevented hypothermia in patients during surgery. The relative expression of vascular  $\alpha$ -receptors was also inhibited by the synthesized compound in a dose-dependent manner. Importantly, the new compound exhibited no toxicity and excellent biocompatibility during disease treatment. Therefore, this compound may be an excellent candidate for the prevention of hypothermia by decreasing the relative expression of vascular  $\alpha$ -receptors with low side effects.

#### Supplementary Data

Supplementary Data associated with this article are available in the electronic form at [http://nopr.niscair.res.in/jinfo/ijca/IJCA\\_60A\(12\)1557-1563\\_SupplData.pdf](http://nopr.niscair.res.in/jinfo/ijca/IJCA_60A(12)1557-1563_SupplData.pdf).

#### Reference

- 1 Brown D J A, Brugger H, Boyd J & Paal P, *N Engl J Med*, 367 (2012) 1930.
- 2 Peiris A N, Jaroudi S & Gavin M, *JAMA*, 319 (2018) 1290.
- 3 Fernandes T A, Costa I F M, Jorge P, Sousa A C, André V, Cerca N & Kirillov A M, *ACS Appl Mater Interfaces*, 13 (2021) 12836.
- 4 Hu M L, Abbasi-Azad M, Habibi B, Rouhani F, Moghanni-Bavil-Olyaei H, Liu K G & Morsali A, *ChemPlusChem*, 85 (2020) 2397.
- 5 Hu M L, Razavi S A A, Piroozzadeh M & Morsali A, *Inorg Chem Front*, 7 (2020) 1598.
- 6 Hu M L, Masoomi Y M & Morsali A, *Coord Chem Rev*, 387 (2019) 415.

- 7 Fan L, Zhao D, Li B, Wang F, Deng Y, Peng Y, Wang X & Zhang X, *Spectrochim Acta A*, 264 (2022) Article 120232.
- 8 Fan L, Zhao D, Zhang H, Wang F, Li B, Yang L, Deng Y & Zhang X, *Micropor Mesopor Mat*, 326 (2021) Article 111396.
- 9 Wang F, Tian F, Deng Y, Yang L, Zhang H, Zhao D, Li B, Zhang X & Fan L, *Cryst Growth Des*, 21 (2021) 4242.
- 10 Ran H P, Du H L, Ma C Y, Zhao Y Y, Feng D N & Xu H, *Sci Adv Mater*, 13 (2021) 741.
- 11 Bharati A K, Somnath, Lama P & Siddiqui K A, *Inorg Chim Acta*, 500 (2020) Article 119219.
- 12 Liu C Y, Chen X R, Chen H X, Niu Z, Hirao H, Braunstein P & Lang J P, *J Am Chem Soc*, 142 (2020) 6690.
- 13 Chen D M & Zhang X J, *J Solid State Chem*, 278 (2019) Article 120906.
- 14 Rouhani F, Rafizadeh-Masuleh F & Morsali A, *J Mater Chem A*, 7 (2019) 18634.
- 15 Xiao Q Q, Dong G Y, Li Y H & Cui G H, *Inorg Chem*, 58 (2019) 15696.
- 16 Zheng L N, Wei F H, Hu H M, Bai C, Yang X L, Wang X & Xue G, *Polyhedron*, 161 (2019) 47.
- 17 Sanati S, Abazari R, Morsali A, Kirillov A M, Junk P C & Wang J, *Inorg Chem*, 58 (2019) 16100.
- 18 Liang X, Jia Y, Zhan Z & Hu M, *Appl Organomet Chem*, 33 (2019) e4988.
- 19 Liu X, Xu Y, Deng Y & Li H, *Cell Physiol Biochem*, 46 (2018) 1439.
- 20 Duncan R & Izzo L, *Adv Drug Deliv Rev*, 57 (2005) 2215.